CASE REPORT

Patrick M. Grant,[1] Ph.D; Kenton J. Moody,[1] Ph.D.; Ian D. Hutcheon,[1] Ph.D.; Douglas L. Phinney,[1] Ph.D.; Jeffrey S. Haas,[1] M.S.; Alan M. Volpe,[1] Ph.D.; James J. Oldani,[1] M.S.; Richard E. Whipple,[1] B.A.; Nancy Stoyer,[1] Ph.D.; Armando Alcaraz,[1] M.S.; John E. Andrews,[1] M.S.; Richard E. Russo,[1] Ph.D.; Gregory L. Klunder,[1] Ph.D.; Brian D. Andresen,[1] Ph.D.; and Shawn Cantlin,[1] M.S.

Forensic Analyses of Suspect Illicit Nuclear Material

REFERENCE: Grant PM, Moody KJ, Hutcheon ID, Phinney DL, Haas JS, Volpe AM, Oldani JJ, Whipple RE, Stoyer N, Alcaraz A, Andrews JE, Russo RE, Klunder GL, Andresen BD, Cantlin S. Forensic analyses of suspect illicit nuclear material. J Forensic Sci 1998;43(3):680–688.

ABSTRACT: A small metal sample, alleged to be a substance that could substitute for highly enriched uranium in a nuclear weapon, was subjected to qualitative and quantitative forensic analyses using methods of materials science, radioisotopic chemistry, inorganic chemistry, and organic chemistry. The specimen was determined to be moderately pure Sc, likely derived from a uranium refining operation. Although no fissionable species or weaponization signatures were detected, the sample did exhibit some unusual properties. These anomalies included lanthanide fractionation, with concentrations of Dy, Ho, and Er elevated by factors greater than 100 over normal levels, and the presence of long, odd-chain fatty acids.

KEYWORDS: forensic science, illicit nuclear materials, nuclear smuggling, nuclear forensic analyses and characterization

Since the end of the Cold War and the fragmentation of the former Soviet Union (FSU) into independent states several years ago, concerns have been raised about the present and future security of nuclear weapons and other fissile materials within the FSU. Increasing potential for the black-market availability of highly enriched uranium (HEU) and weapons-grade plutonium (^{239}Pu) has focused international attention on the danger of nuclear proliferation by rogue nations, as well as on nuclear terrorism (1,2). Most of the instances of nuclear smuggling to date have involved scams or sales of nonexplosive radioactive materials (3), but law-enforcement seizures of such non-weapons-grade materials have become commonplace throughout Europe. These species have included nuclides such as depleted-^{238}U (advertised as HEU), ^{241}Am from smoke-detector alarms, and other industrial isotopes (such as ^{60}Co and ^{137}Cs).

However, since 1992, there have been a number of confirmed cases in which kilogram quantities of HEU and Pu were stolen from existing stockpiles of special nuclear material (4,5). This increasing diversion of weapons- or near-weapons-quality resources from national inventories has resulted in calls for new disposal methods during warhead dismantlement, and for enhanced nuclear safeguards procedures in general (6,7).

The enhanced threat of diversion of weapons-grade materials has fostered increased credibility with respect to a number of nuclear hoaxes. One such scam that has led to forensic analyses of suspect samples in our laboratory is the ''red mercury'' phenomenon. This substance has been asserted to provide a strategic ingredient for nuclear bombs, allegedly allowing the ignition of a fusion secondary without the necessary acquisition of HEU or ^{239}Pu as a primary fission trigger. Red mercury has also been variously promoted as an integral component of anti-radar coatings, gravity bombs, medicines, and missile guidance systems. The selling price of the purported material is on the order of $500,000 per kg (8).

Black-market sales of red mercury are often accompanied by incredible data for the physical properties of the substance. With specific reference to Fig. 1, for example, a density of 20.2 g/cm^3 would be greater than that of all but the platinum-group elements, the claim of an ''isotopic temperature'' of 160°C is quite novel, other listed parameters are nonsense, and listing Lawrencium as a transuranic, actinide impurity suggests the overthrow of several laws of nature. The longest-lived, known isotope of Lawrencium is ^{262}Lr, with a half-life of approximately three hours. Lr nuclei are extremely difficult to produce and require heavy-ion bombardment of an actinide target to generate a few atoms at any one time; there are no pathways for the production of Lr isotopes by neutron-capture reactions in reactors or accelerators. Moreover, any Lr activities successfully synthesized will decay to extinction within a maximum time of about one day.

Such technical inaccuracies are routinely found in frauds involving the illicit trafficking of nuclear materials. Our analytic experience with purported red mercury specimens to date has been consistent with those samples being nothing more than elemental Hg, HgO, or HgI_2.

However, a somewhat more tenable, nuclear-related sample with an illicit association was recently submitted to our laboratory for analyses. It was a small piece of gray metal in an empty 35-mm film container that federal law enforcement had acquired during a recent investigation. The specimen was said to be representative of a larger quantity of material that could be used instead of HEU

[1]Deputy director, radiochemist, materials scientist, materials scientist, chemist, chemist, metallurgist, chemist, radiochemist, chemist, chemist, laser specialist, chemist, director, and nuclear engineer, respectively, Forensic Science Center, L-178, Lawrence Livermore National Laboratory, Livermore, CA.

Received 23 July 1997; accepted 26 Sept. 1997.

INQUIRY:

MERCURY 20 . 20

COMPLETE CHEMICAL ANALYSES OF RED MERCURY 20.20.

DENSITY	:	20.20 G/CM^3
FORMULA	:	Sb2 O7 Hg2
TOTAL MOL. WEIGHT	:	755/757 GRAM/MOL.
MOLECULAR WEIGHT	:	196.0127 ± 0.02 G/MOL
PURITY	:	99.95 TO 99.99 % PROOF
COLOUR	:	CHERRY RED OR BURGUNDY RED
FORM	:	LIQUID AT P0=1.01325 BAR
MELTING POINT	:	-37.070° C
FLASH POINT	:	170.026° C
BOIL. POINT	:	350.720° C
TEMP. ISOTOPIC	:	160.070° C
RADIO ELEMENT NAT.	:	SF 6 SIC APPROX. N° 0.794
FS GAMMA	:	0.440 - 0.439
REACTION K	:	0.00016 - 0.00015
REACTION P	:	9.000 - 8.000
REACTION ABSOL.TEMP	:	0.062
REACTION VIT TEMP.	:	1.024
REACTION VDSA	:	0.29 - 0.30
REACTION RFN	:	0.744 OR 0.794
HANDLING	:	THE SUBSTANCE IS WEAKLY RADIOACTIVE. SAFE FOR MANIPULATION AND HANDLING.
FLASKS	:	NY 19 OR NY 22
DATE OF PRODUCTION	:	LESS THAN 90 DAYS

SPECTRAL ANALYSIS:

SUBJECT: RED MERCURY - STANDARD RED 20.20 (CONTENTS OF ELEMENTS IN %)

Cr 1 * 10^{-7}	Cu 1 * 10^{-7}	Sn 1 * 10^{-8}
Ni 1 * 10^{-7}	Pb 3 * 10^{-7}	Co 2 * 10^{-7}
Ag 1 * 10^{-8}	Mg 1 * 10^{-7}	Al 1 * 10^{-7}

TRANSURANIUM - ACTINIDA: LAURENCIUM Lr - 103

ISOTOP STRUCTURE:

O 16 - 99.76 %	Hg 198 - 10.20 %	Hg 201 - 13.22 %
O 17 - 0.037 %	Hg 199 - 16.80 %	Hg 202 - 29.80 %
O 18 - 0.20 %	Hg 200 - 23.10 %	Hg 204 - 6.80 %
Hg 196 - 0.16 %		

FIG. 1—*Technical specifications sheet for ''red mercury'' 20.20.*

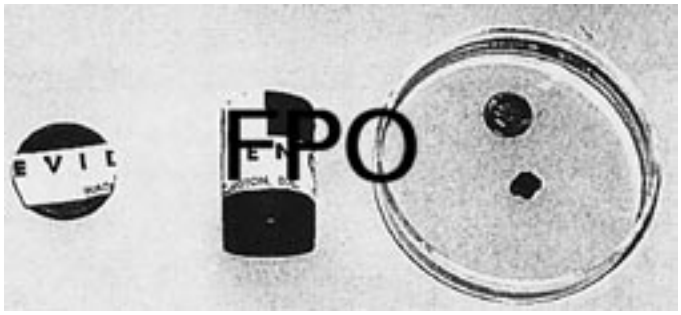

FIG. 2—*Suspect nuclear material and a U.S. dime in a Petri dish, along with the outer container (a 35-mm film canister).*

in a nuclear weapon. Law enforcement requested forensic characterization of this sample, and we describe our applied technology and ensuing results in this paper.

Materials and Methods

Nondestructive Analyses and Sample Partitioning

The specimen and 35-mm film container are shown in Fig. 2. The questioned sample weighed 0.3713 g, with dimensions approximately 8.9 mm × 8.2 mm × 3 mm thick. The two flat sides of the specimen had different and distinct surface morphologies. One side, which we designated ''A,'' had a prominent cut mark and rough features (see Fig. 3*a*). The other, designated ''B,'' had smoother characteristics and a bubbled surface (see Fig. 3*b*).

We performed nondestructive nuclear and atomic analyses (NDA) on the entire specimen. Gas proportional counters were employed to interrogate both flat surfaces for gross-α and gross-β radioactivities. The sample was also counted for 20 h on a high-efficiency, low-background, 4096-channel Ge spectrometer system

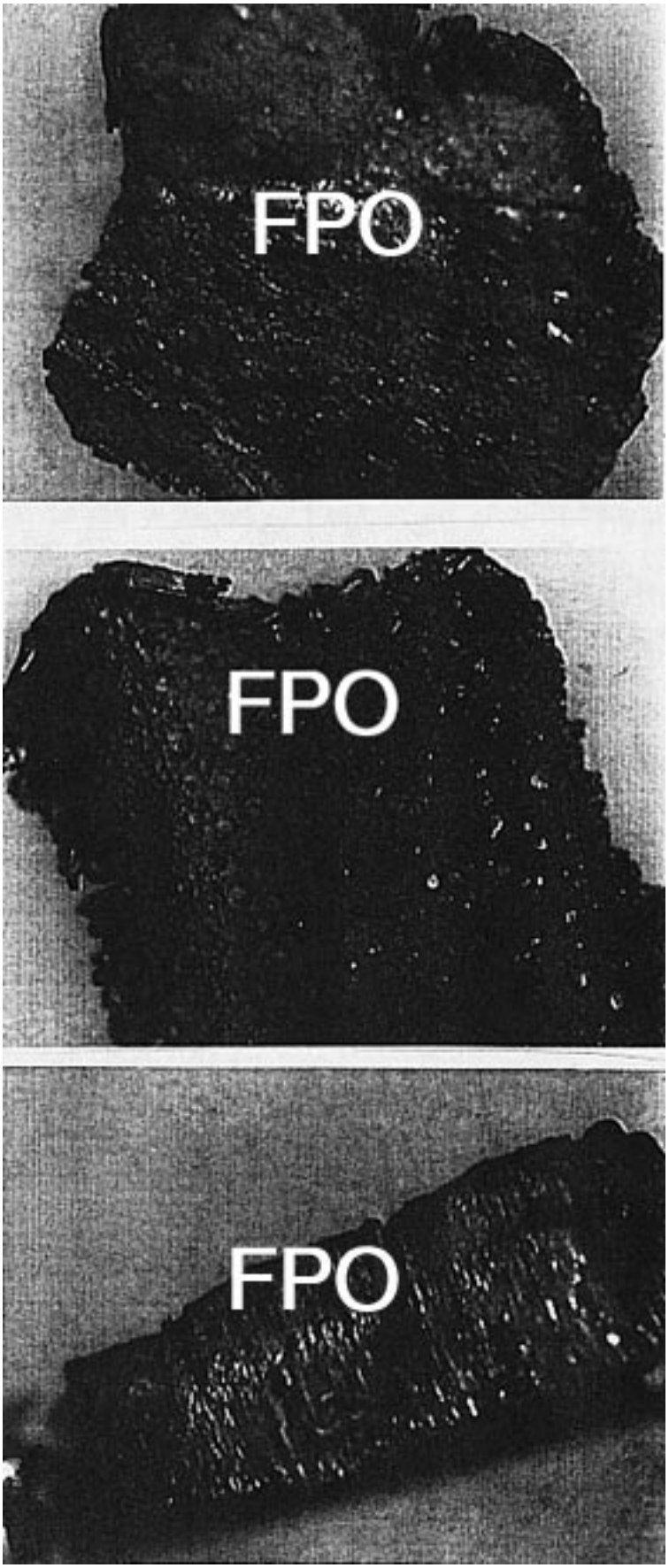

FIG. 3—*Photomicrographs (~10×) of sample surfaces: (a)* (top) *as-defined side A; (b)* (middle) *as-defined side B; (c)* (bottom) *edge-on view.*

for any γ emission between 50–2000 keV. All of these nuclear NDA measurements gave results that were indistinguishable from the normal background signals of the various analyzers.

We then performed qualitative, elemental examinations of the specimen's surfaces by X-ray fluorescence (XRF) analyses using a ^{109}Cd isotopic excitation source. Side A was determined to be composed primarily of the metal scandium (Sc), with a small presence of Fe and trace Mo also observed. Surface B was likewise predominantly Sc, but it additionally contained readily detectable quantities of Fe, Cr, and Ni, along with trace Mo.

The specimen was next sonicated and extracted multiple times with a solvent system consisting of ultrapure 3:1 methylene chloride/isopropanol. The interior of the film canister was similarly treated, and these extraction solutions were set aside for organic analyses by gas chromatography-mass spectrometry (GC-MS).

Using a diamond blade with deionized-water lubricant, we then partitioned a portion of the sample for destructive analyses. The material was somewhat difficult to cut and actually broke one blade. The pieces thus obtained for further investigations were 95.6 mg for forensic radiochemistry, 60.5 mg for electron microscopy and electron- and ion-microprobe analyses, 30.3 mg for quantitative elemental analysis by inductively-coupled-plasma mass spectrometry (ICP-MS), and 15.0 mg for metallurgy. We returned the remainder of the specimen to law enforcement for further analyses or archival storage.

Metallurgy and Microprobe Analyses

Backscattered electron imaging and wavelength-dispersive quantitative chemical analyses of the sample were performed with a JEOL-733 automated electron microprobe. The instrument produced a focused electron beam of 15 keV and 10–20 nA for this study. Pure metal (Sc, V, Cr, Fe, Ni, Mo) and Ca-phosphate standards were used, and characteristic X-ray intensities were converted to analyte concentrations by means of a Sandia Task ZAF algorithm. Acquisition times for minor elements were typically 30–60 s, which produced minimum detection limits on the order of 0.01 wt%.

We performed sensitive elemental and isotopic analyses of the sample by ion-microprobe mass spectrometry (9). The Cameca IMS-3f ion microscope is a sputtering-source mass spectrometer with micron-scale imaging capability. As a secondary-ionization mass spectroscopy (SIMS) instrument, it provided detection capability for the isotopes of every element of the periodic table. Through the implementation of suitable standards, determinations were made of isotopic ratios and elemental abundances to detection limits of 0.01–10 parts-per-million (ppm) by weight. The ion microscope used sample amounts on the order of pg to μg, and performed the analyses *in situ.* The *in situ* character of SIMS analysis requires no sample preparation (or processing) other than mounting. This capability permits selective analyses of distinct phases of heterogeneous samples.

Forensic Radiochemistry

The sensitive determination of diagnostic nuclear signature species requires extensive and complex radiochemical decontamination procedures for each element of interest, followed by nuclear-decay or mass-spectrometric assays of purified chemical fractions. Such methods have been developed for isotopes of the heavy elements Ra, Ac, Th, Pa, U, Np, Pu, Am, and Cm, and we implemented these procedures for the present investigation. Details of these methods are available elsewhere (10–12).

Organic Analyses

We performed organic analyses using a Hewlett-Packard model 5890 gas chromatograph interfaced to a Hewlett-Packard model 5988 quadrupole mass spectrometer. The GC was equipped with a 30-m, Alltech SE-30, methyl silicone capillary column, having an i.d. of 0.25 mm and a 0.25-μm film thickness. A splitless injection mode was used, with a 1-min residence time at 250°C. The temperature program for the oven encompassed a 10-min hold-time at 70°C, followed by a ramp at 8°C per minute to 320°C. Data acquisition began at 0.01 min for the underivatized samples and at 9.5 min for the derivatized samples.

The mass spectrometer was operated in electron-impact mode (70 eV and ~300 μA), with the source temperature at 200°C and interface temperature at 300°C. The tuning compound used for MS calibration was perfluorotributylamine [PFTBA, $(C_4F_9)_3N$]. The default ions used for the tuning procedure were m/z = 69, 219, and 502 amμ, with their standardized ratios approximately 100%, 45%, and 2.5%, respectively. The full-width-half-maximum (FWHM) relative peakwidths at 69 and 502 amu were constant at ±0.1 amμ. In addition, a standard mixture of Programmed Test Mix (13) was analyzed to evaluate the MS sensitivity and monitor column performance.

After concentration by evaporation, 2-μL aliquots of the organic solvent used to extract the specimen and the film canister were injected into the GC-MS for qualitative analyses. Because polar organic compounds are typically not amenable to direct GC analysis using methyl silicone columns, we subjected aliquots of the samples to derivatization with N,O-bis(trimethylsilyl)trifluoroacetamide (BSTFA) to improve the GC-MS characterization. A 250-μL aliquot was introduced into an open 4-mL vial, placed in a Reacti-Therm evaporator at 20°C, and evaporated to dryness using a stream of 99.999%-pure He. Approximately 100 μL of BSTFA were added to cover any residual material. The Teflon screw-cap was tightened, and the vial was then heated for 60 min at 60°C in the Reacti-Therm. Two-μL aliquots were then injected into the GC-MS for assay of additional polar compounds present on the specimen and the film container.

We identified each individual compound in a GC-MS total-ion chromatogram by means of a computerized, National Institute of Standards and Technology (NIST) library search and comparison with known compounds. Individual interpretation of mass-spectral data was also employed.

Inorganic Analyses

The 30-mg subsample was dissolved in concentrated, ultrapure mineral acid, and all sample preparation was done under Class 100-1000 cleanroom conditions using ultrapure reagents and Teflon labware. The dissolved specimen was slowly evaporated to near-dryness in an Ar-flushed Teflon evaporation unit under a heat lamp. The sample was then treated twice with conc. HNO_3, followed by evaporation to dryness. The resultant residue was dissolved in 0.5 M HNO_3 and subjected to instrumental analysis. A procedural blank was treated identically.

Using ICP-MS, we performed sensitive, multielement atomic analyses, spanning the range from mass Z = 3 (Li) to Z = 94 (Pu). The instrument was a modified VG/Fisons Plasmaquad model operated at an incident RF power of 1350 w with <5 w reflected. Argon gas-flow rates were 12.0 L/min for the plasma, 0.7 L/min auxiliary, and 0.85 L/min for the Meinhard, Type-C nebulizer. Sample uptake rate was 0.63 mL/min, and ion pulse-counting was performed via an ETP model AF563 system operating at 2550 V

and 20-ns deadtime. Data were collected in a 4096-channel analyzer, which spanned the mass range from 5.5–240 amμ.

For the ICP-MS analyses, we employed a 45-element external standard with analyte concentrations of 1, 10, or 100 ng/g (ppb). External standards determined a linear calibration curve for the calculation of analyte concentrations, while three elements (Ga, In, and Tl) were employed as internal standards. Reported concentrations were therefore corrected for instrument drift, matrix-suppressed analyte responses, and other analytic errors. We determined minor- and trace-element concentrations of 42 atomic species, with detection limits established for an additional 3 elements.

Results and Discussion

Metallurgy and Electron Probe Analyses

Metallurgical analysis of the sample indicated that it was likely residual material from a casting pour. Domains of long, columnar grain growth with some oxide inclusions, and no evidence of dendritic structures, were characteristic of the specimen. Such grain structure would be expected from solidification of a larger cast piece of relatively pure material. These domains gave the appearance of a bundle of thin metal wires, ~0.1–0.3 mm in diameter, sintered to form a dense, coherent assembly (see Fig. 4*a*). However, the porosity of the sample was very low, and the diameter of individual grains was not uniform.

An individual domain is shown in Fig. 4*b*; the exterior surface exhibited linear features parallel to the grain axis. This surface was free of contamination except for occasional 2–5 μm chips of Ta. One end of each column grain appeared to have been cut, while the other end was rounded and covered with μm-sized pits (Fig. 4*c*). The latter morphology suggested that this end was perhaps part of a molten front, or had been exposed to a chemically reactive environment.

This rounded and pitted tip exhibited significant amounts of Cr, Fe, and Ni. To characterize the chemical variability of the material, electron microprobe traverses were performed on a freshly cut surface oriented normal to the surface with the rounded tips. A total of five traverses were performed, using a 5-μm step size to cover a 500-μm-wide region extending inward from the outer surface; the orientation of these traverses was parallel to the grain axis. Chemical compositions were also measured at ~75 randomly

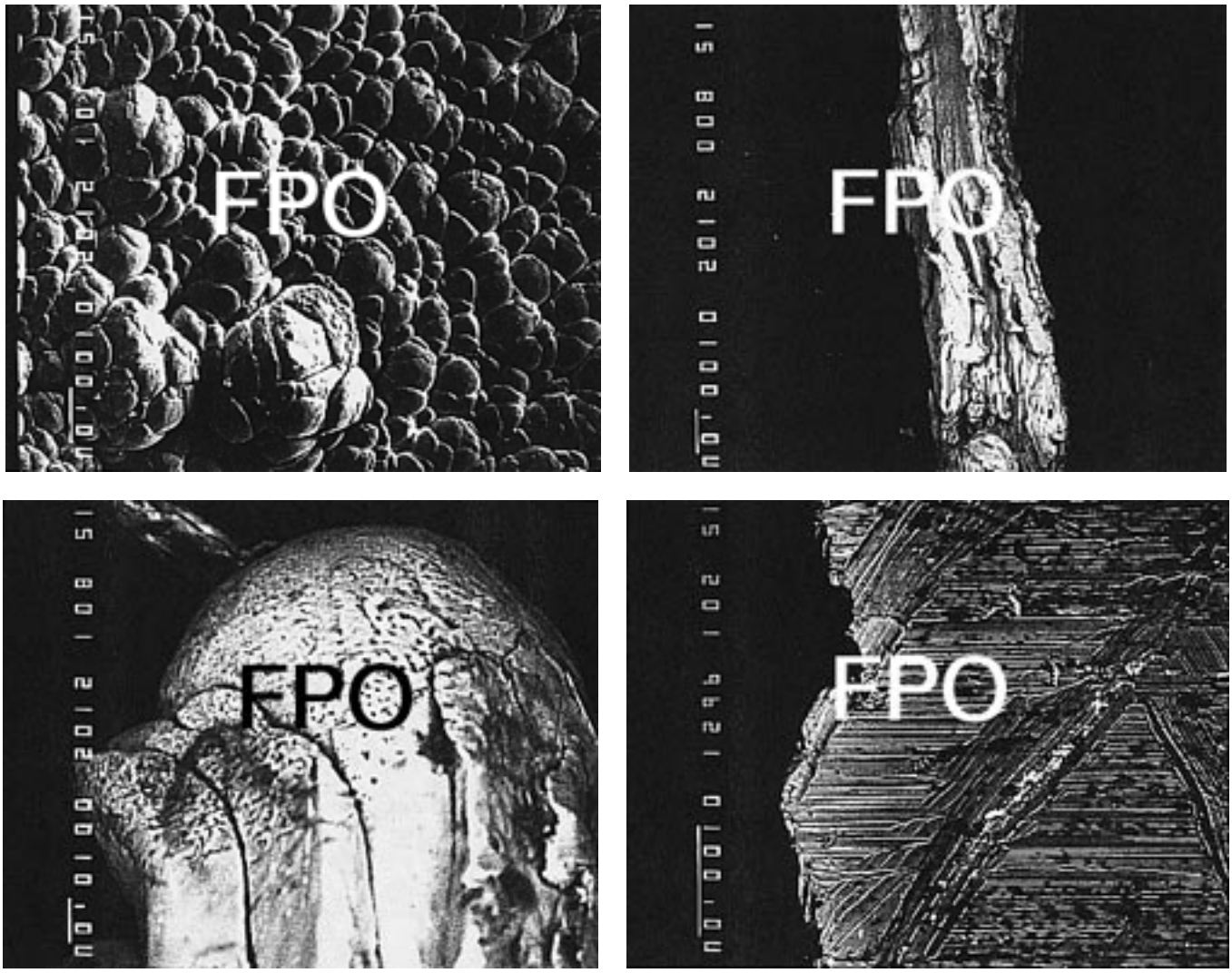

FIG. 4—*Electron probe photomicrographs of:* (a) *end-on view of sample surface showing individual domains of columnar grain growth;* (b) *side view of a separated grain;* (c) *rounded tip of a separated grain;* (d) *cross-sectional view. The exterior surface enriched in Cr and Fe is at the top edge of* 4d*, and the electron probe traverses represented in Fig. 5 were performed parallel to the striations visible in* 4d.

TABLE 1—*Composition of interior and surface regions of the specimen, determined by electron microprobe. See text for description of ''interior'' and ''surface'' locations. Uncertainties are 2σ.*

Element	Interior Concentration (weight %)	Surface Concentration (weight %)
Sc	99.59 ± 0.18	86.06 ± 0.60
P	0.29 ± 0.02	0.29 ± 0.05
V	<0.01	0.02 ± 0.01
Cr	0.06 ± 0.01	5.18 ± 0.35
Fe	0.08 ± 0.02	8.24 ± 0.45
Ni	0.01 ± 0.01	0.23 ± 0.10
Mo	<0.02	<0.02
Total	100.03	100.02

spaced points located >600 μm from this surface. Following these analyses, the specimen was reoriented, and the chemical composition of the rounded-tip surface was obtained directly. We summarize the results of these measurements in Table 1 and Fig. 5.

The concentrations of Sc, Cr, Fe, and Ni were strongly zoned in the outer 0.6-mm region of the sample. The Sc concentration was inversely related to those of Cr, Fe, and Ni, increasing with increasing distance away from the rounded tip and further into the interior of the specimen. The abundances of Cr, Fe, and Ni were highest at the outer-tip surface (Cr ~5 wt%, Fe ~8 wt%, and Ni ~ 0.2 wt%) and fell off rapidly with increasing distance into the center, decreasing by factors of ~5 over the initial 150 μm.

Although they displayed roughly similar behaviors, the five traverses could be divided into two groups on the basis of location. Traverses 1 and 2 (Fig. 5*a*) exhibited more gradual decreases of Fe and Cr with increasing distance than traverses 3–5 (Fig. 5*b* and 5*c*). The two sets of traverses were separated by 0.5 mm, normal to the traverse direction. Localized ''hot spots,'' containing up to 12 wt% Fe and 8 wt% Cr, were observed in the outer 100 μm (Fig. 5*a*); one central ''hot spot,'' containing little Fe or Cr but >0.5 wt% Ni, was also measured. These ''hot spots'' were most plausibly attributed to μm-size metallic inclusions. Despite the large variation in chemical compositions, the Fe/Cr ratio remained relatively constant, gradually increasing from ~1.5 at the surface to ~2 at a depth of 0.3 mm. The Fe/Ni ratio decreased from ~40 at the surface to ~5 over this same distance.

Beyond a depth of ~0.6 mm, regular variations in composition were absent; for discussion purposes, we define this region as the ''interior'' of the specimen. The sample interior was moderately high-purity Sc, with the major impurity being P. In contrast to the transition metals, the P concentration was uniform throughout the sample at ~0.3 wt%. Neglecting occasional ''hot spots,'' Cr, Fe, and Ni appeared relatively homogeneous within the interior; together they summed to a total concentration of ~0.15 wt%.

Since the interior of the specimen contained little Fe, Cr, or Ni, we concluded that the elevated concentrations of these elements at the tip surface indicated diffusion-controlled chemical transport from a Cr-Fe-Ni-rich material, and that the relative abundances of these elements reflected an environment to which the sample was exposed (and perhaps that in which it was cast). However, in contrast to the metal compositions used for common stainless steels, the contacting material or environment of the specimen was characterized by a much lower Fe/Cr ratio (~1.5) and a much higher Fe/Ni ratio (~40). The uniform distribution of P throughout the specimen suggested an intimate association of P with Sc, possibly

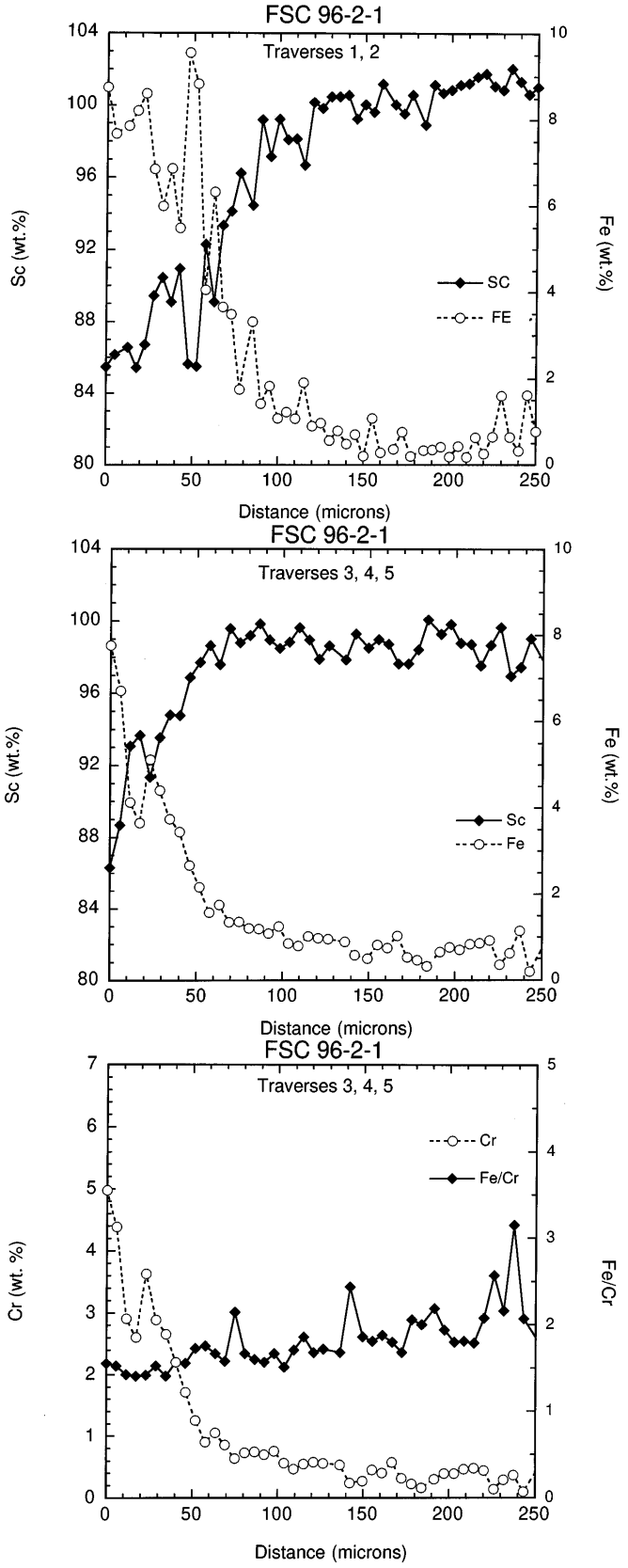

FIG. 5—*Chemical composition of the sample as a function of distance from the surface, determined by electron microprobe:* (a) *variation of Sc and Fe concentrations along traverses 1 and 2 in the outer 250 μm;* (b) *variation of Sc and Fe concentrations along traverses 3, 4, and 5 in the outer 250 μm; variation of Cr concentration and the Fe/Cr ratio along traverses 3, 4, and 5 in the outer 250 μm.*

TABLE 2—*Forensic radiochemistry results for the specimen. Activity data are disintegrations per minute per gram of sample; errors are 1σ.*

Nuclide	A (dpm/g)
^{226}Ra	2.6 ± 1.7
^{228}Th	0.74 ± 0.53
^{229}Th	≤0.64
^{230}Th	2.21 ± 0.74
^{232}Th	≤0.53
^{234}U	≤14
^{235}U	1.6 ± 1.4
^{238}U	≤15
^{237}Np	≤3.6
^{238}Pu	≤1.8
^{239,240}Pu	≤1.8

arising from incomplete chemical separation during Sc refining operations.

Nuclear Forensic Analyses

The results of α-particle and γ-ray analyses of separated radiochemical fractions are given in Table 2. At the 95% confidence level, we observed evidence for only one radioactive signature: ^{230}Th. Definitely present in the questioned specimen, ^{230}Th is not independently abundant, but is found in nature only as a daughter-product of the decay of naturally occurring uranium. This analysis indicated that the sample was associated with U at some time during its history, but no evidence of any weaponization activities was detected.

SIMS and ICP-MS Elemental Analyses

The combined results of trace-element analyses of the sample, by both ICP-MS and SIMS, are given in Table 3. The measured concentrations of 52 inorganic analytes are presented in units of μg/g of sample (ppm), and the reported data are the means of five separate measurements. The ICP-MS values were quantitative determinations, with estimated relative uncertainties of ~1–2% or better for the higher-concentration analytes, and ~20% for lower-concentration species. The ion microprobe analyses were also quantitative, and their estimated errors were ~20%.

These elemental data indicated that P, Cr, Fe, and Ni were present at levels above what might be expected in routine materials [e.g., by comparison with concentrations of elements present in the earth's crust (14)]. The Cr, Fe, and Ni analytes could have arisen through surface contact and diffusional contamination by a corrosion-resistant Fe alloy at elevated temperature. However, either the composition of such an alloy was quite different from those of normal stainless steels, or multiple steels and differential fractionation of metallic components may have been involved.

The elevated P in the sample was an additional indication that the specimen was perhaps derived from U mining or processing operations. Uranium has historically been recovered industrially as a by-product from wet-process phosphoric acid refining procedures, and P-containing reagents [such as tributyl phosphate, di-(2-ethylhexyl) phosphoric acid, and trioctylphosphine oxide] have often been used for refinement by solvent extraction (15). Most commercial Sc is recovered from the minerals thortveitite or cassiterite, or is extracted as by-product from U mill tailings. One procedure for isolating Sc from the leach liquors of U refining chemistry incorporates additional extraction, precipitation, and calcination steps (16,17). The extractant used is dodecyl phosphoric acid, also a P-containing solvent.

TABLE 3—*Minor- and trace-element composition of the sample. Data measured by ICP-MS, except microprobe values indicated by ''*.'' See Text for discussion of error estimates (1σ).*

Element	Abundance (ppm)	Element	Abundance (ppm)
Li	<0.001	Cd	0.03
Be	2.8	Sn	12*
B	0.28	Sb	0.06
C	2400*	Te	0.01
F	62*	Cs	0.1
Na	18*	Ba	0.71
Mg	2.6	La	0.82
Al	290*	Ce	1.8
Si	460*	Pr	0.4
P	2900*	Nd	11
Cl	950*	Sm	0.02
K	72*	Eu	0.004
Ca	12*	Gd	0.7
V	<0.001	Tb	0.9
Cr	1200	Dy	32
Mn	120	Ho	16
Fe	1800	Er	33
Co	1.8	Tm	0.08
Ni	220	Yb	0.01
Cu	54	Lu	0.33
Zn	1.2	Hf	0.14
As	<0.001	Ta	0.2
Rb	0.45	W	0.51
Sr	0.09	Pb	11
Y	5.4	Bi	0.22
Zr	0.29	Th	0.32
Nb	0.13	U	0.15
Mo	1.3		

TABLE 4—*Lanthanide distribution data, normalized to [La], for meteoritic, crustal, reference-standard, and sample materials. See text for discussion.*

Ln	Chondrites (18)	Earth's Crust (14)	NIST-1632a (19)	USGS AGV-1 (19)	Sample	Sample/ terrestrial
La	1.00	1.00	1.00	1.00	1.00	1
Ce	2.7	2.0	1.9	1.7	2.2	1
Pr	0.35	0.27	—	—	0.49	2
Nd	1.9	0.93	0.80	0.89	13	10
Sm	0.57	0.20	0.16	0.16	0.024	0.1
Eu	0.21	0.040	0.035	0.044	0.005	0.1
Gd	0.76	0.18	0.17	0.14	0.85	5
Tb	0.14	0.03	0.02	0.02	1.1	50
Dy	0.97	0.10	0.14	0.10	39	300
Ho	0.23	0.04	—	—	20	500
Er	0.59	0.09	—	—	40	400
Tm	0.09	0.02	—	—	0.10	5
Yb	0.65	0.10	0.07	0.04	0.012	0.2
Lu	0.10	0.02	0.01	0.007	0.40	30

The measured lanthanide (Ln) distribution pattern in the sample was quite anomalous. Because of their nearly identical reaction behaviors, Ln species do not significantly fractionate during natural chemical, biologic, or geologic transformations, even over long time scales (18). Since they retain group coherence within diverse environments, Ln elements have found many applications as geochemical markers. Table 4 lists Ln distribution data, normalized to the concentration of La, for primordial chondrite abundances

(18), the earth's crust (14), two standard reference materials (19), and the questioned specimen. The last column gives the ratio of the measured sample datum to the average of the three terrestrial values for each Ln species.

The relative concentrations of Dy, Ho, and Er were very elevated in the sample, indicating an introduction of chemically separated Ln species at some time during its history. The forensic interpretation of this finding is equivocal. Few practical uses have been found for Ho, while Dy has been used in nuclear disciplines for neutron-control applications because of its high capture cross-section. However, Er has found recent use in the nuclear industry (20), and erbia (Er_2O_3) is presently used as a mold wash for some metal casting operations. If pressed to propose an origin for the peculiar Ln distribution in the questioned specimen, we could speculate that erbia might have been used to wash a crucible sometime before the subsequent introduction of the sample, and that the chemical purification of Er from neighboring rare-earth elements was more indicative of a practical-grade material than that of an analytic reagent. However, this speculation would be relatively uncertain.

Organic Analyses

The GC-MS data resulting from the extractions of the sample and the film-canister container were reasonably complex. Figures 6 and 7 show the total-ion chromatograms of the underivatized and derivatized extracts, respectively, of the specimen. Approximately 100 peaks were examined for identification in these combined spectra, and a similar number were scrutinized in the derivatized and underivatized solvent from the film canister. Those compounds extracted from the specimen and identified, and which were not similarly found on the plastic film container, are listed in Table 5.

The underivatized GC-MS spectra from both the metal and the container extractions were characterized by the presence of plasticizers and oxidized, long-chain hydrocarbons. Such species are derived from synthetic, rather than natural, processes. The derivatized spectrum of the specimen displayed a number of long, even- and odd-chain fatty acids. The even-carbon-number acids are indicative of a biologic origin (21), whereas the odd-chain acids result principally from synthetic procedures. The odd long-chain fatty acids were unusual in that they have rarely been observed in our past analyses of forensic samples. Other atypical compounds on the sample were the C_{18} alcohol and butylated species, as well as the two nitriles. Our interpretation of these GC-MS results is that the data reflect a mixture of two general sources of organic materials. Some of the detected molecules likely resulted from human handling, while others were synthetic species of unknown origin.

Conclusions

The questioned specimen was comprised of reasonably pure Sc metal; the major impurity in the bulk sample was P at ~0.3 wt%. An exterior surface was enriched in Cr (~5 wt%), Fe (~8 wt%), and Ni (~0.2 wt%), and the concentrations of these elements decreased rapidly with depth, reaching interior levels within 300

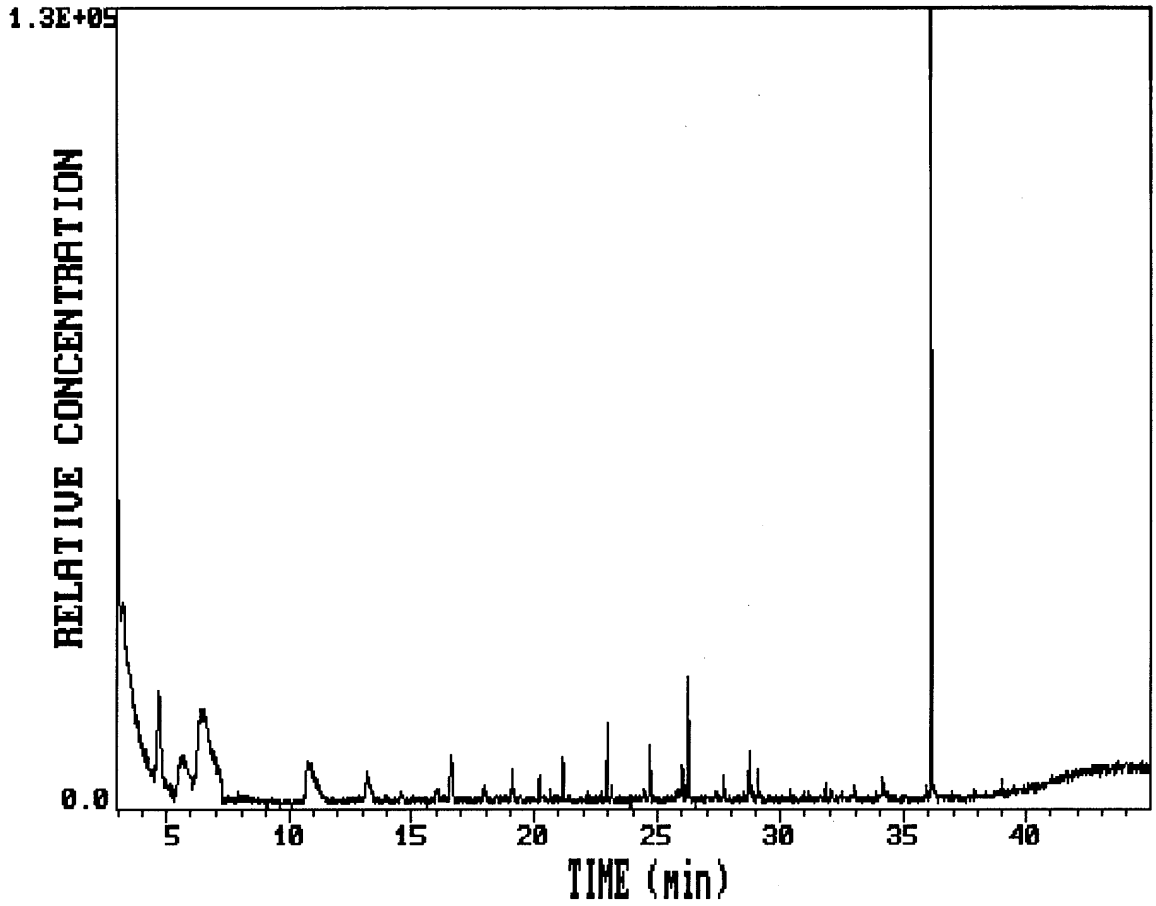

FIG. 6—*GC-MS total-ion plot of the underivatized extraction solvent of the specimen.*

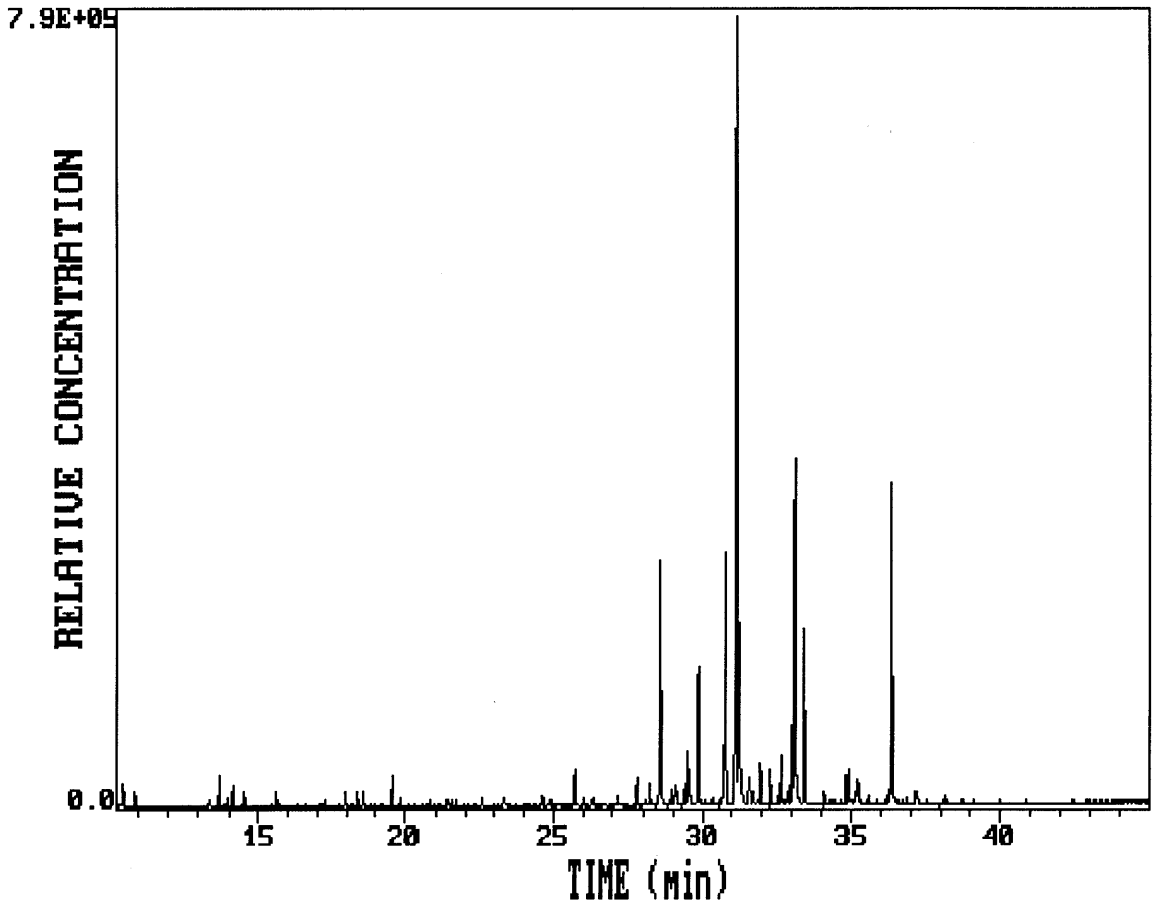

FIG. 7—*GC-MS total-ion plot of the extraction solvent of the specimen after derivatization with BSTFA.*

TABLE 5—*Organic species extracted from the sample alone and analyzed by GC-MS. Compound identifications based on library database and individual interpretations of MS data.*

Compound	Retention Time* (min)
Underivatized	
3,3,5-trimethylheptane	15.76
octadecanal	26.26
bis(2-ethylhexyl)phthalate	36.09
Derivatized	
undecanitrile	26.02
tridecanoic acid	27.18
tetradecenoic acid	28.22
tetradecanoic acid	28.56
hexadecanitrile	28.93
5-hydroxy-1H-indole-2-carboxylic acid	29.52
dibutylphthalate	29.57
palmitoleic acid	30.78
heptadecanoic acid	32.29
octadecanol	32.53
9,12-octadecadienoic acid	33.02
octadecanoic acid	33.44
butyl ester of octadecanoic acid	34.90
dioctylphthalate	36.36

*See text for GC analysis conditions.

μm. The most likely origin of the sample was from the side of a crucible, possibly made of a corrosion-resistant Fe alloy, after pouring a casting mold. A trace quantity of ^{230}Th signature indicated a definite prior association with natural U, although only 0.15 ppm residual U remained in the sample. It is therefore quite possible that the specimen derived from a uranium mine and had been subsequently refined by chemical processing. However, HEU, Pu, or other fissionable species were not detected in the sample, nor was the presence of any other weaponization indicators. Whereas Sc is chemically similar to the lanthanides and actinides, its nuclear properties are not, and its purported use as surrogate bomb material was clearly a hoax.

We measured several interesting anomalies in the specimen. The rare-earth distribution pattern was very unusual, with the relative concentrations of Dy, Ho, and Er elevated by more than two orders of magnitude. This extreme Ln fractionation may have resulted from an erbia mold wash of a crucible subsequently utilized to refine the sample. In addition, several odd-carbon-number, long-chain fatty acids were present on the specimen. These species were unusual for forensic samples, and they indicated possible inputs from one or more synthetic processes.

Acknowledgments

This work was performed under the auspices of the U.S. Department of Energy by Lawrence Livermore National Laboratory under contract W-7405-ENG-48. The interest in, and support of, nuclear

forensic analyses by Michael F. O'Connell, DOE Office of Nonproliferation and National Security, is gratefully acknowledged. The authors are also grateful for technical editing of this work by Lori A. McElroy.

References

1. Nuckolls JH. Post-cold war nuclear dangers: proliferation and terrorism. Science 1995;267:1112–4.
2. von Hippel F. Fissile material security in the post-cold-war world. Phys Today 1995;48(6):26–31.
3. Williams P, Woessner PN. The real threat of nuclear smuggling. Sci Amer 1996;274(1):40–4.
4. Stone R. German lab points the way in hunt for 'hot' plutonium. Science 1994;265:1355–6.
5. Hileman B. Nuclear theft poses growing security threat. Chem Eng News 1995;11 September:24–5.
6. Speed RD. The international control of nuclear weapons. Stanford Univ:Center for International Security and Arms Control, 1994.
7. Hileman B. U.S. and Russia face urgent decisions on weapons plutonium. Chem Eng News 1994;13 June:12–25.
8. Hogsett V. Red mercury: caveat emptor. Washington, DC: Department of Energy/Office of Nonproliferation Technology Support; Critical Technologies Newsletter 1992: DOE/ONTS-92-010-001.
9. Zinner E. Depth profiling by secondary ion mass spectrometry. Scanning 1980;3:57–78.
10. Moody KJ. Dissolved oralloy standards and the origin of HEU. Livermore, CA: Lawrence Livermore National Lab. 1994; UCRL-ID-117611.
11. Moody KJ. Determination of plutonium metal origins. Livermore, CA: Lawrence Livermore National Lab. 1995; UCRL-ID-120253.
12. Moody KJ. Forensic radiochemistry of PUBLIC site inspection samples. Livermore, CA: Lawrence Livermore National Lab. 1995; UCRL-ID-119658.
13. Grob K Jr, Grob G. Comprehensive, standardized quality test for glass capillary columns. J Chromatog 1978;156:1–20.
14. Lide DR, editor. CRC handbook of chemistry and physics. 73rd edition. Baca Raton, FL: CRC Press, 1992–93;14–7.
15. Weigel F. Uranium. In: Katz JJ, Seaborg GT, Morss LR, editors. The chemistry of the actinide elements. 2nd edition. London: Chapman and Hall, 1986;(1):169–442.
16. Lash LD, Ross JR. Scandium recovery from uranium solutions. J Metals 1961 August:555–8.
17. McGinley FE, Facer JF. Uranium as a by-product and by-products of uranium production. In: Uranium ore processing. Vienna: International Atomic Energy Agency, STI/PUB/453, 1976;181–90.
18. Laul JC. Rare earth element behavior in the development of energy resources. Proceedings of the Fifth International Conference on Nuclear Methods in Environmental and Energy Research; CONF-840408; Washington, DC: U.S. Dept. of Energy Technical Information Center, 1984;426–37.
19. Ewa IOB, Elegba SB, Adetunji J. Rare earth element patterns in Nigerian coals. J Radioanal Nucl Chem, Lett 1996;213(3):213–24.
20. Office of Nonproliferation and National Security. Nuclear terms handbook—1996. Washington, DC: U.S. Dept. of Energy, 1996; 76.
21. Chalmers RA, Lawson AM. Organic acids in man. London: Chapman and Hall, 1982.

Additional information and reprint requests:
Pat Grant
Forensic Science Center, L-178
Livermore National Laboratory
Livermore, CA 94550